

# Selecting cold 2n transfer in $^{162}\text{Dy}(^{116}\text{Sn}, ^{118}\text{Sn})^{160}\text{Dy}$

T. Härtlein, H. Bauer, D. Pansegrau, D. Schwalm

Max-Planck-Institut für Kernphysik, D-69117 Heidelberg, Germany

Received: 4 September 1998

Communicated by B. Povh

**Abstract.** Cold 2n transfer has been studied using the reaction  $^{162}\text{Dy}(^{116}\text{Sn}, ^{118}\text{Sn})^{160}\text{Dy}$  at energies in the vicinity of the Coulomb barrier. The experiment was performed at the Heidelberg-Darmstadt Crystal Ball spectrometer which was extended by 6 Compton suppressed Ge-detectors. It is demonstrated, that the direct population of intrinsically cold states in the deformed  $^{160}\text{Dy}$  transfer product can be selected by identifying and suppressing excitations to states above the yrast line using the Crystal Ball. The probability for populating yrast states in the deformed  $^{160}\text{Dy}$  nuclei in a 2n transfer reaction increases from 7 % at grazing collisions up to  $\approx 50$  % at large impact parameters, while the probability for populating the ground state in the spherical 2n transfer product  $^{118}\text{Sn}$  stays about constant at  $\approx 45$  % for all measured impact parameters.

**PACS.** 25.70.Cd Elastic and quasielastic scattering and transfer

## 1 Introduction

Enhanced correlated transfer of nucleon pairs in grazing collisions of two superfluid heavy nuclei has been extensively studied in recent years [1-5]. This so-called pairing enhancement, proposed in the early 70's by Dietrich et al. [6], is expected to occur between nuclei that exhibit strong pairing correlations. Ideal candidates for studying neutron pairing are the stable even-even mid-shell Sn nuclei. When investigating 2n transfer reactions between these spherical nuclei, an enhancement factor of  $10^2 - 10^3$  relative to DWBA values was observed for the transfer between the ground states of even Sn nuclei  $0^+, 0^+ \rightarrow 0^+, 0^+$  [4,7], which is in agreement with transfer calculations including pairing [8].

Extending the correlated pair transfer investigations to deformed nuclei, one should be able to study the modifications of the pairing correlations due to deformation and rotation. For heavy spherical nuclei impinging on well deformed nuclei, like  $^{116}\text{Sn} \rightarrow ^{162}\text{Dy}$ , Coulomb excitation of the members of the rotational band built on the ground state of the deformed nucleus, which form the yrast sequence of these nuclei up to spins around  $16\hbar$ , will always accompany the reaction. Since the Coulomb force is of long range while the nucleon transfer peaks around the turning point of the quasi-elastic scattering trajectory, the transfer takes place when the deformed nucleus has already acquired a certain rotational angular momentum. Calculations [9,10] show, that for well deformed nuclei the angular momentum near the turning point is rather well defined within a few  $\hbar$  and can be shifted up and down by choosing an appropriate kinematic of the quasi-

elastic scattered ions. Thus, by measuring the correlated 2n pair transfer leading to yrast states in the deformed transfer product  $^{160}\text{Dy}$  (*cold* transfer) under various kinematic conditions, it should be possible to gain information about the pairing correlations as a function of rotational frequency and their quenching caused by the Coriolis force. Furthermore, due to the nuclear deformation an increasing influence of transfer multipolarities other than  $L = 0$  is expected, resulting in distinct modifications of the 2n transfer cross sections for individual yrast states of the deformed nucleus [11]. Experimental evidence for such modifications has been claimed in different scattering systems using  $^{12}\text{C}$  [12,13] or  $^{116}\text{Sn}$  projectiles [14] impinging on well deformed rare earth nuclei.

In scattering systems involving deformed nuclei, however, uncorrelated transfer to high lying quasiparticle states (*hot* transfer) is the dominating process. In order to study the 2n transfer leading from the yrast states of the initial nucleus to the yrast states of the transfer product one therefore has to have a sensitive method to distinguish cold and hot transfer events. As this is a critical prerequisite for any further studies concerning correlated pair transfer involving deformed nuclei, the main aim of the present investigation was to demonstrate a technique for selecting cold transfer events in reactions like  $^{162}\text{Dy}(^{116}\text{Sn}, ^{118}\text{Sn})^{160}\text{Dy}$ .

To be more precise, the events we would like to select are — in analogy to the  $0^+, 0^+ \rightarrow 0^+, 0^+$  transfer studies between spherical nuclei mentioned above — the 2n transfer leading from an yrast state of the initial deformed nucleus  $A$  to an yrast state of the final deformed nucleus  $A \pm 2$  (see Fig. 1) with the initial and final spherical col-

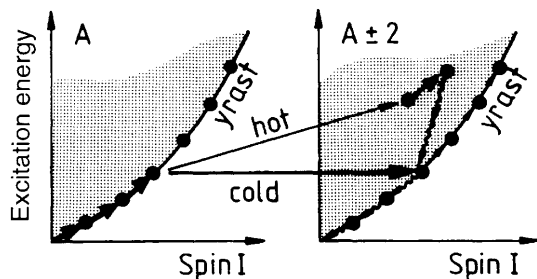


**Fig. 1.** On the definition and selection of cold 2n transfer events. Coulomb excitation takes place before and after the transfer process

lision partner  $B$  and  $B \mp 2$  remaining in their respective  $0^+$  ground states. Due to the Coulomb excitation taking place before the transfer process, however, not only the ground state (yrast-) band of  $A$  is excited but also collective surface vibrations built on the ground state of  $A$  as well as of  $B$ . Although the ground state band excitations will dominate, the contributions from vibrational excitations cannot be disregarded in these transfer studies. On the other hand, as long as one is primarily interested in investigating the pairing correlations as a function of rotation and deformation, we may as well extend our selection criteria for *cold* transfer events by allowing for collective surface vibrations in the initial *and* final channels, as these excitations are expected to preserve the pairing correlations of the corresponding ground states. For the collision system studied in the present investigation cold transfer events may thus involve the first excited  $2_1^+$  states in the spherical Sn nuclei as well as the  $\gamma$ -bands in the deformed Dy-isotopes.

To shed more light on the cold transfer process in heavy collision systems involving deformed nuclei we will also be interested in transfer processes where one of the reaction products stays in its ground state or ground state band, respectively, while the excitation of the other product is disregarded. In the following we will refer to these classes of events as *semi-cold* transfer events to distinguish them from the (true) *cold* transfer events defined above.

Before and after the transfer process the selection criteria for cold transfer events are guaranteed by the selectivity of the Coulomb excitation process. For an event by event decision whether a cold or hot 2n transfer has taken place, however, one has to resolve the final states. Particle spectrometers are not suited because of their small solid angle and because they only allow to determine the total excitation energy with insufficient resolution. Even with an optimal  $Q$  value resolution of 1.5 MeV [5], one can only measure averages over many final states. Essential tools to overcome these restrictions are highly efficient  $4\pi$   $\gamma$ -ray arrays, which allow to determine the individual  $\gamma$ -transition energies as well as the total excitation energy (via the  $\gamma$ -sum energy) and spin  $I$  (via the  $\gamma$ -ray multiplicity) on an event by event basis. As one cannot trigger on cold transfer by gating on individual  $\gamma$ -rays (see also Fig. 1), the strategy is to suppress hot transfer, which asks for an as high as possible total  $\gamma$ -efficiency of the array to optimize its suppression function.

The selection methods developed in the present investigation are used to determine the fraction of cold transfer events, and to study the semi-cold transfer as a function of the impact parameter.

## 2 Experimental method

### 2.1 Experimental details

The experiment was performed by bombarding an  $850 \mu\text{g}/\text{cm}^2$  target highly enriched to 97.5 % in  $^{162}\text{Dy}$  with  $^{116}\text{Sn}$  projectiles provided by the heavy ion accelerator facility at the MPI für Kernphysik in Heidelberg. The isotopic contamination of  $^{160}\text{Dy}$  in the  $^{162}\text{Dy}$  target was measured to be only  $\approx 1.5 \cdot 10^{-3}$ . This allows to estimate contributions from the Coulomb excitation of the contaminating  $^{160}\text{Dy}$ , which cannot be distinguished from the cold 2n pickup transfer. The 2n pickup channel  $^{162}\text{Dy}(^{116}\text{Sn}, ^{118}\text{Sn})^{160}\text{Dy}$ , which has a  $Q_{gg}$  value of +1.6 MeV, was studied at two beam energies of 609 MeV and 639 MeV slightly above the Coulomb barrier. In addition, a calibration run at a 'safe' energy of 509 MeV was carried out, where only Coulomb excitation can take place.

Deexciting  $\gamma$ -rays were measured with the Heidelberg-Darmstadt Crystal Ball [15] consisting of 162 individual NaI-modules, that offers a unique possibility to effectively suppress hot processes and thereby to select cold events due to its high efficiency and  $4\pi$  geometry ( $\varepsilon_{\text{tot}} \approx 95\%$ ). In order to identify the reaction channels by characteristic  $\gamma$  transitions, 6 NaI-modules were replaced by high resolution Ge-detectors with active Compton suppression, adding up to a total Ge-photopeak efficiency of  $\varepsilon_{\text{Ph}}(E_\gamma = 1 \text{ MeV}) \approx 0.1\%$ . A system of 6 parallel plate avalanche counters (PPAC), covering an angular region in the forward hemisphere of  $30^\circ \leq \vartheta_{\text{lab}} \leq 85^\circ$  and  $0^\circ \leq \varphi_{\text{lab}} \leq 360^\circ$  was used to detect target-like and projectile-like nuclei in kinematic coincidences with an angular resolution of  $2^\circ$  and  $3^\circ$  respectively for  $\vartheta_{\text{lab}}$  and  $\varphi_{\text{lab}}$ . Therefore, the PPAC array allows to reconstruct Rutherford-like trajectories assumed for quasi-elastic collisions in the center of mass angular region from  $\theta = 60^\circ$  to  $120^\circ$  and to correct for the Doppler shift of the  $\gamma$ -rays. Particle- $\gamma$  coincidence data, demanding at least one  $\gamma$ -ray to be detected in a Ge-detector, were taken as well as scaled down particle singles.

The  $\vartheta$ - $\vartheta$ -correlation and the time-of-flight information of both scattered particles were used to distinguish between projectile-like and target-like reaction products. As deep-inelastic reactions with a total transferred energy of  $E^* \geq 50 \text{ MeV}$  and a transferred mass of  $\Delta m \geq 4 \text{ amu}$  change the Rutherford trajectory in a traceable way, the PPAC information allows in addition for a coarse distinction between quasi-elastic and deep-inelastic reactions. The final selection of quasi-elastic reactions is done with the Crystal Ball by demanding that (i) the measured  $\gamma$ -sum energy is smaller than 10 MeV, (ii) the  $\gamma$ -multiplicity is smaller than 12 and (iii) all NaI-detectors have only prompt time signals, thereby discriminating neutrons from

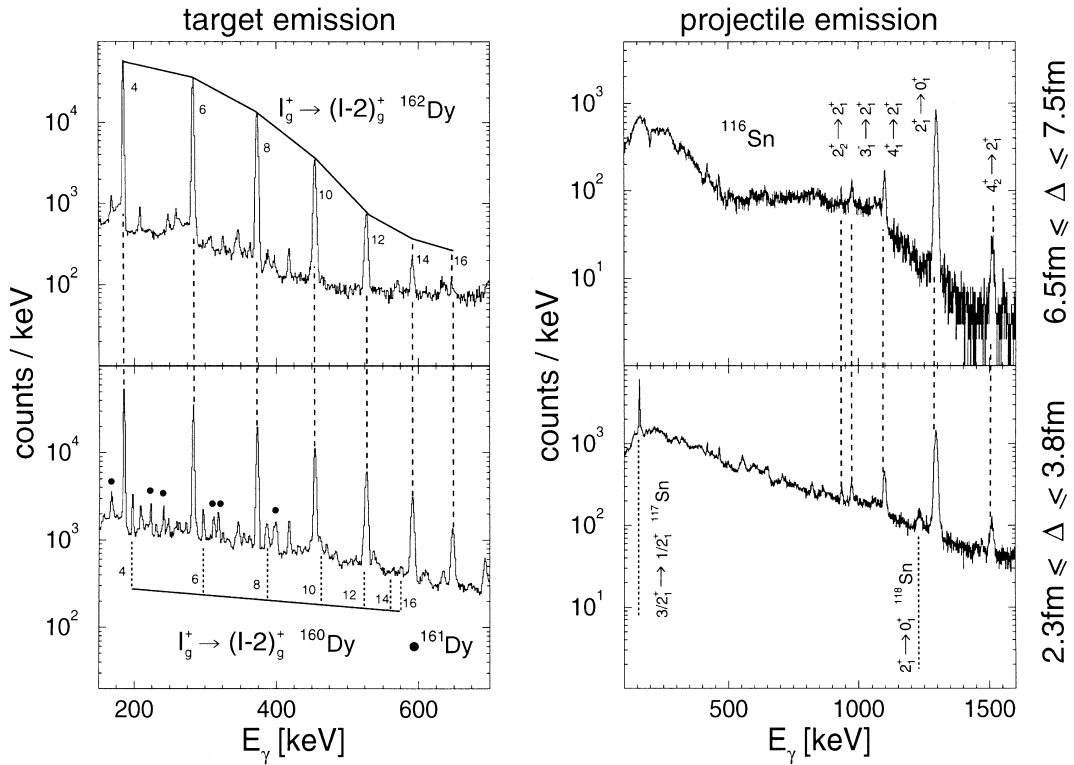


**Fig. 2.** Doppler corrected Ge-spectra, assuming  $\gamma$ -ray emission from target-like (left panel) or projectile-like nuclei (right panel) at safe distances of  $6.5 \text{ fm} \leq \Delta \leq 7.5 \text{ fm}$  (upper spectra) and at reaction distances of  $2.3 \text{ fm} \leq \Delta \leq 3.8 \text{ fm}$  (lower spectra)

$\gamma$ -rays via their different time of flight. From the symmetry of the Crystal Ball time spectra after applying condition (i) and (ii) one can conclude, that together with cut (iii) contributions of events accompanied by neutron evaporation can be kept below 5 % even for the smallest impact parameters.

To quantify the distance of the surfaces of the two colliding nuclei at the turning point, we shall use in the following a generalized surface distance  $\Delta(\theta_{\text{cm}})$  [16] defined by

$$\Delta(\theta_{\text{cm}}) = D(\theta_{\text{cm}}) - (C_1 + C_2). \quad (1)$$

$D(\theta_{\text{cm}})$  is the distance of closest approach between the centroids of the two colliding nuclei as a function of the scattering angle  $\theta_{\text{cm}}$ , and  $C_i$  are the radii of the diffuse Fermi mass distribution of the two colliding nuclei with

$$C_i = R_i(1 - R_i^{-2}) \text{ [fm]} \quad \text{and} \quad (2)$$

$$R_i = 1.28A_i^{1/3} - 0.76 + 0.78A_i^{-1/3} \text{ [fm]}. \quad (3)$$

Since the surface diffuseness of nuclear mass distributions is almost constant for heavy nuclei, the surface distance  $\Delta$  is to a great extent independent of the mass of the two nuclei and therefore an appropriate measure of the nuclear overlap. Distances of  $\Delta > 6.5 \text{ fm}$  are generally regarded as 'safe' distances [16], where nuclear contributions to excitation probabilities are less than a few percent. With decreasing distance, the nuclear overlap increases and nucleons start to be exchanged. The region  $2.3 \text{ fm} \leq \Delta \leq$

$3.8 \text{ fm}$ , which corresponds to grazing collisions leading to the maximum of the transfer cross section, will be called below the 'reaction distance' region.

The possibility of selecting the kinematics via the PPAC array and thereby the possibility to vary the nuclear overlap is nicely visible in Fig. 2, which shows Ge-spectra for quasi-elastic events at safe distances (upper spectra) and at reaction distances (lower spectra). The Doppler correction of the measured  $\gamma$ -rays is performed assuming that the  $\gamma$ -rays are emitted either by the target-like Dy ('target emission') or projectile-like Sn nuclei ('projectile emission'). The spectra corrected for projectile emission were not incremented, if the measured energy — after Doppler correction assuming target emission — corresponded to a yrast transition in  $^{162}\text{Dy}$ . Thus, wrongly corrected yrast transitions in  $^{162}\text{Dy}$ , which would lead to broad lines dominating the projectile-corrected spectra at low energies are avoided. At safe distances only transitions in the Coulomb excited  $^{162}\text{Dy}$  and  $^{116}\text{Sn}$  nuclei are visible in Fig. 2. In the target-corrected Ge-spectrum the yrast transitions of  $^{162}\text{Dy}$  up to  $16_g^+ \rightarrow 14_g^+$  can be identified, whereas in the projectile-corrected spectrum the lowest transitions in  $^{116}\text{Sn}$  are visible. At reaction distances, in addition, transitions of the transfer products of the 2n ( $^{160}\text{Dy}$  and  $^{118}\text{Sn}$ ) and 1n pickup channel ( $^{161}\text{Dy}$  and  $^{117}\text{Sn}$ ) can be observed. The stripping as well as other transfer channels are strongly suppressed because of their unfavorable negative  $Q_{gg}$  values of  $-3 \text{ MeV}$  and below.

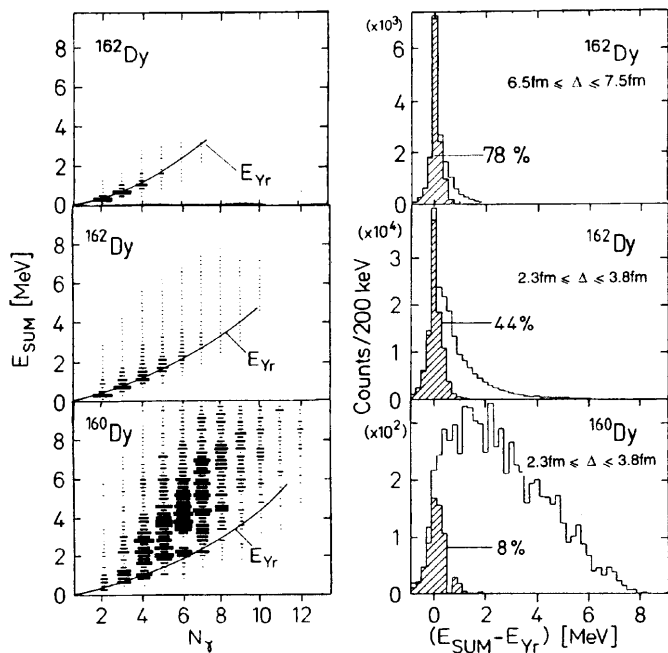


**Fig. 3.**  $\gamma$ -sum energy vs.  $\gamma$ -multiplicity (left panel) and the 'yrast projections' (right panel, see text) for the Coulomb excitation channel at safe distances  $6.5\text{ fm} \leq \Delta \leq 7.5\text{ fm}$  (top), at reaction distances  $2.3\text{ fm} \leq \Delta \leq 3.8\text{ fm}$  (middle), and for the 2n transfer channel at reaction distances (bottom). All  $\gamma$ -rays are Doppler corrected assuming target emission. The shaded projections are obtained if events are selected where no  $\gamma$ -ray with  $E_\gamma > 720$  keV was observed (see also text)

## 2.2 Selection of cold events

The left panels of Fig. 3 show for different event types the correlations of the  $\gamma$ -sum energy  $E_{\text{sum}}$  (assuming target emission) versus the  $\gamma$ -multiplicity  $N_\gamma$  of the  $\gamma$ -rays detected in the Crystal Ball and the Ge-detectors. All prompt  $\gamma$ -rays were considered in an event with one possible exception: A  $\gamma$ -ray corresponding to the  $2_1^+ \rightarrow 0^+$  yrast transition in  $^{116}\text{Sn}$  (1.294 MeV) or  $^{118}\text{Sn}$  (1.230 MeV) after Doppler correction for projectile emission is disregarded and taken out of the event. These transitions are therefore not included in the spectra shown in Fig. 3 and are not subjected to later energy cuts. This procedure allows to retain events where the first excited  $2_1^+$  state in the Sn-like nuclei has been excited. The Coulomb excitation and the 2n pickup channel were selected by gating on the  $4_g^+ \rightarrow 2_g^+$  or  $6_g^+ \rightarrow 4_g^+$  transition in  $^{162}\text{Dy}$  and  $^{160}\text{Dy}$ , respectively, detected in one of the Ge-detectors. The upper and the middle spectrum correspond to the Coulomb excitation channel at safe distances and at reaction distances, respectively. As expected from the increasing interaction strength at smaller surface distances, the population of higher yrast states as well as the increased population of states above the yrast line  $E_{\text{Yr}}$  is clearly visible in Fig. 3. The bottom spectrum corresponds to the 2n pickup channel at reaction distances. The yrast line for  $^{160}\text{Dy}$  indicated in this spectrum was obtained from a corresponding Coulomb excitation measurement on a  $^{160}\text{Dy}$

target. While a large fraction of the population in the Coulomb excitation channel leads directly to yrast states, it is obvious that the 2n pickup channel mainly populates states with energies 2 – 3 MeV above the yrast line, with an increasing tendency for increasing spins, i.e. most of the observed 2n transfer is hot. The population above the yrast line is illustrated in a more quantitative way on the right hand side of Fig. 3 which displays the projection of the  $E_{\text{sum}}$  vs.  $N_\gamma$  plane along lines of constant energy above the yrast line ('yrast projection').

In order to select cold events on an event by event basis, we make use of the fact that a direct population of an yrast state in the Dy-like nucleus is followed only by yrast transitions with energies below  $\approx 700$  keV for all conceivable yrast states ( $I \leq 18$ ). Therefore an event is assumed to be cold if no energy signal with  $E_\gamma > 720$  keV was detected (neither in the Crystal Ball nor in the Ge-detectors). Moreover, events involving excited levels in the Sn nuclei other than the first excited  $2_1^+$  state (the corresponding  $2_1^+ \rightarrow 0^+$  decay being taken out of the event) are equally well suppressed by this energy cut. The effect of this  $E_\gamma \leq 720$  keV condition is shown in Fig. 3 by the dashed histograms in the 'yrast projections'. The remaining symmetric peaks around zero indicate that this cut selects indeed events in which the yrast sequences in the Dy nuclei have been directly populated. It is moreover obvious from Fig. 3 that this selection method, which is based on the detection of individual  $\gamma$ -rays, is more effective than a cut along the yrast line in the  $E_{\text{sum}}$  vs.  $N_\gamma$  plane, the latter criterion being unable to suppress events accidentally lying on the yrast line due to undetected  $\gamma$ -rays.

The fraction of events, where no  $E_\gamma > 720$  keV  $\gamma$ -ray was detected, decreases for Coulomb excitation events from  $(78 \pm 2)\%$  at safe distances to  $(44 \pm 1)\%$  at reaction distances and drops to  $(8 \pm 2)\%$  for 2n pickup events, the large error of the last value being due to the statistics of the  $^{160}\text{Dy}$  gating transitions in the Ge-spectrum. Especially in the 2n pickup channel, however, part of the selected events may be still due to hot events because of the finite  $\gamma$ -detection efficiency of the setup. To estimate this contribution we have to consider the efficiency for detecting an  $E_\gamma > 720$  keV  $\gamma$ -ray ( $\varepsilon(E_\gamma > 720\text{ keV}) \approx 0.7$ ) and the observed multiplicity distribution for  $E_\gamma > 720$  keV  $\gamma$ -rays. For the 2n pickup channel at reaction distances, the average observed multiplicity is  $N_\gamma(E_\gamma > 720\text{ keV}) \approx 2$  with tails up to  $N_\gamma(E_\gamma > 720\text{ keV}) = 5$ . Taking this into account the fraction of true cold 2n pickup events, i.e. of events where both reaction partners remain cold, reduces to only  $(3 \pm 2)\%$ . For the Coulomb excitation channel, this correction is less dramatic and the fractions reduce from 78% to 74% and from 44% to 38% at safe and reaction distances, respectively.

In contrast to the Sn nuclei, where we explicitly allow for the population of the first  $2_1^+$  vibrational states in the selection cut for cold events, events leading to a population of the  $\gamma$ -vibrational bands in the Dy nuclei, which decay to the yrast band by emitting  $\gamma$ -rays in the energy region between 0.7 MeV to 1.2 MeV are also suppressed by the

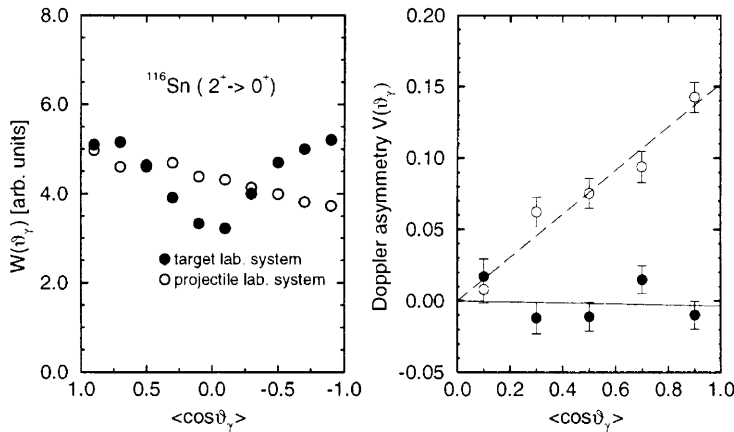


**Fig. 4.** Angular distribution  $W(\vartheta_\gamma)$  and Doppler asymmetry  $V(\vartheta_\gamma)$  of the  $2_1^+ \rightarrow 0^+$  transition in  $^{116}\text{Sn}$ , analysed in the target and projectile lab. system, respectively

$E_\gamma \leq 720$  keV condition. Unfortunately this cannot be avoided because by increasing the energy cut to 1.2 MeV the suppression power for the dominating hot events in the 2n pickup channel at reaction distances is significantly spoiled; in fact, by requiring  $E_\gamma > 1.2$  MeV, the selected 'cold' events were found to increase by a factor of two whereas only an increase of about 30 % is expected.

The fraction of only 3 % of cold 2n pickup events as compared to the total 2n pickups at surface distances of  $2.3 \text{ fm} \leq \Delta \leq 3.8 \text{ fm}$  is surprisingly small. It underlines the need for a very selective and efficient method if one is aiming at a detailed investigation of cold 2n transfer events involving deformed nuclei. The method proposed in the present chapter seems to be able to meet these requirements provided the efficiency of the Ge-part can be considerably increased without spoiling the overall  $\gamma$ -efficiency of the setup. Due to our limited Ge-efficiency in the present experiment, we were not able to investigate these cold 2n transfer events in more detail. To get nevertheless more insight into the transfer process involving heavy and deformed collision partners, we shall select and discuss below semi-cold transfer events, which were defined in Sect. 1.

### 2.3 Selection of semi-cold events

To determine the number of events, where the ground state band in  $^{160}\text{Dy}$  was directly populated, disregarding the excitation of  $^{118}\text{Sn}$  (semi-cold Dy transfer events), we exploited the effect of the Doppler transformation on the  $\gamma$ -angular distribution to deduce the relative percentage of the  $\gamma$ -rays with  $E_\gamma > 720$  keV which are emitted by the target- or projectile-like nucleus.

This so-called Doppler asymmetry analysis can be nicely demonstrated using the  $2_1^+ \rightarrow 0^+$  transition in the Coulomb excited  $^{116}\text{Sn}$ . In a laboratory system where the  $z$ -axis coincides with the recoil direction of the projectile-like nucleus (projectile lab. system), the angular distribution of this  $\gamma$ -transition is distorted due to the Lorentz transformation of the solid angle  $d\Omega_\gamma^{\text{lab}} = (1 + 2\beta_p \cos \vartheta_\gamma^p) d\Omega_\gamma^{\text{rest}}$ . Here,  $\beta_p$  denotes the velocity of the recoiling projectile-like nuclei and  $\vartheta_\gamma^p$  the polar angle of

the emitted  $\gamma$ -rays in the projectile lab. system. This distortion results in an asymmetry  $V^p(\vartheta_\gamma^p)$  with respect to  $\vartheta_\gamma^p = 90^\circ$  of the polar angular distribution  $W^p(\vartheta_\gamma^p)$ , which can be quantified by the so-called Doppler asymmetry parameter  $A^p$ :

$$V^p(\vartheta_\gamma^p) = A^p \cos \vartheta_\gamma^p \equiv \frac{W^p(\vartheta_\gamma^p) - W^p(180^\circ - \vartheta_\gamma^p)}{W^p(\vartheta_\gamma^p) + W^p(180^\circ - \vartheta_\gamma^p)} \quad (4)$$

In case of the  $2_1^+ \rightarrow 0^+$  transition of  $^{116}\text{Sn}$ , the Doppler asymmetry parameter in the projectile lab. system is simply given by  $A^p = 2\beta_p$ . The open circles in Fig. 4 present the polar angular distribution function  $W^p(\vartheta_\gamma^p)$  of the  $2_1^+ \rightarrow 0^+$  transition and the Doppler asymmetry  $V^p(\vartheta_\gamma^p)$  for events taken at  $E_{\text{lab}} = 639$  MeV and at  $\Delta = 3.3$  fm, i.e. for  $\beta_p = 0.074$ . From the measured values an asymmetry parameter of  $A^p = 0.15 \pm 0.01$  has been extracted, which is in excellent agreement with the expected value of  $A^p = 0.148$ . Considering the same  $\gamma$ -transition in a laboratory system, where the  $z$ -axis coincides with the recoil direction of the target-like nucleus (target lab. system), i. e. analysing

$$V^t(\vartheta_\gamma^t) = A^t \cos \vartheta_\gamma^t \equiv \frac{W^t(\vartheta_\gamma^t) - W^t(180^\circ - \vartheta_\gamma^t)}{W^t(\vartheta_\gamma^t) + W^t(180^\circ - \vartheta_\gamma^t)} \quad (5)$$

only a very small Doppler asymmetry is expected, since the angle between the  $z$ -axis of the target and projectile system,  $\zeta_{\text{pt}}$ , is close to  $90^\circ$  due to the rather symmetric scattering system. The filled circles in Fig. 4 represent the angular distribution  $W^t(\vartheta_\gamma^t)$  and Doppler asymmetry  $V^t(\vartheta_\gamma^t)$  of the  $2_1^+ \rightarrow 0^+$  transition of  $^{116}\text{Sn}$  when analysed in the target lab. system, where a pronounced E2 angular distribution but no asymmetry with respect to  $\vartheta_\gamma^t = 90^\circ$  is visible. The extracted Doppler asymmetry parameter is  $A^t = -0.003 \pm 0.011$ , in reasonable agreement with the expectation of  $A^t = 2\beta_p \cos \zeta_{\text{pt}} = -0.025$  for  $\zeta_{\text{pt}} = 100^\circ$ .

In the general case, where the observed  $\gamma$ -rays are either emitted from the projectile-like (fraction  $\lambda$ , average velocity  $\beta_p$ ) or from the target-like reaction product (fraction  $(1 - \lambda)$ , average velocity  $\beta_t$ ), the Doppler asymmetry parameters  $A^p$  and  $A^t$  defined by (4) and (5) are expected to be given by (assuming that the projectile- and target-like nuclei emit their  $\gamma$ -rays on the average isotropically

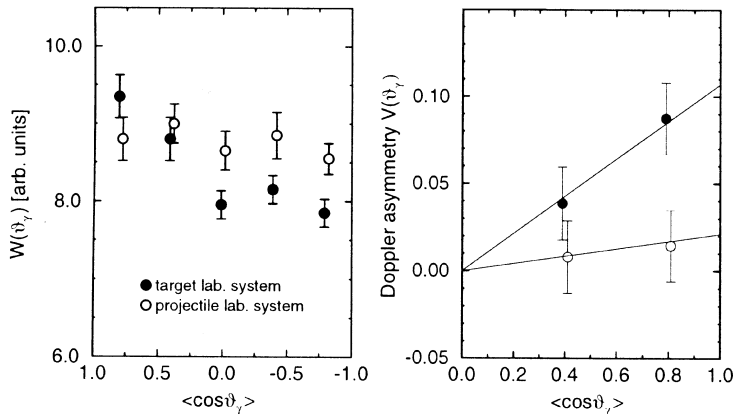


**Fig. 5.** Angular distribution  $W(\vartheta_\gamma)$  and Doppler asymmetry  $V(\vartheta_\gamma)$  of all  $E_\gamma > 720$  keV  $\gamma$ -rays in the 2n pickup channel (with the exception of the  $2_1^+ \rightarrow 0^+$   $\gamma$ -transition in  $^{118}\text{Sn}$ ) at reaction distances  $2.3 \text{ fm} \leq \Delta \leq 3.8 \text{ fm}$

in the respective rest systems, see [17] for more details):

$$A^p = 2(\lambda\beta_p + (1-\lambda)\beta_t \cos \zeta_{pt}) \quad (6)$$

$$A^t = 2((1-\lambda)\beta_t + \lambda\beta_p \cos \zeta_{pt}). \quad (7)$$

Figure 5 displays the  $W(\vartheta_\gamma)$  and  $V(\vartheta_\gamma)$  distributions for  $\gamma$ -rays with  $E_\gamma > 720$  keV connected with the 2n transfer channel leading to  $^{160}\text{Dy}$  and  $^{118}\text{Sn}$  at reaction distances  $2.3 \text{ fm} \leq \Delta \leq 3.8 \text{ fm}$ . Note that the  $^{118}\text{Sn}(2_1^+ \rightarrow 0^+)$  transitions have again been taken out of the events and thus do not contribute to  $W(\vartheta_\gamma)$  or  $V(\vartheta_\gamma)$ . Fitting the two Doppler asymmetries  $V^p(\vartheta_\gamma^p)$  and  $V^t(\vartheta_\gamma^t)$  by  $V(\vartheta_\gamma) = A \cos \vartheta_\gamma$  (Fig. 5, right panel) and using (6) and (7) together with  $\beta_p = 0.070$ ,  $\beta_t = 0.071$  and  $\zeta_{pt} = 101^\circ$ , we find consistently in both coordinate systems that on the average  $\lambda = (28 \pm 7)$  % of the remaining  $E_\gamma > 720$  keV  $\gamma$ -rays are emitted by  $^{118}\text{Sn}$ . Up to a distance of  $\Delta \approx 6$  fm no significant change of this fraction has been observed.

Using  $\lambda = 0.28 \pm 0.07$  and assuming the emission of  $E_\gamma \geq 720$  keV  $\gamma$ -rays from the projectile and target like nuclei to be independent, the fraction of semi-cold 2n transfer events leading to yrast states in  $^{160}\text{Dy}$  regardless of the excitation of  $^{118}\text{Sn}$  are found to be  $(7 \pm 3)$  % at reaction distances ( $2.3 \text{ fm} \leq \Delta \leq 3.8 \text{ fm}$ ).

The reliability of the Doppler asymmetry procedure was tested by applying it also to the Coulomb excitation channel, where the fraction  $\lambda$  of  $E_\gamma > 720$  keV  $\gamma$ -rays emitted by the projectile can be alternatively determined by measuring the individual non-yrast transitions in the Ge-detectors. This spectroscopic method can be used in Coulomb excitation, as the non-yrast yield is focussed in well known states which are coupled to the ground state in  $^{116}\text{Sn}$  or to the ground state band in  $^{162}\text{Dy}$  by large E2 or E3 matrix elements. Applying both methods to the Coulomb excitation channel, the fraction  $\lambda$  was found to be independent of the surface distance  $\Delta$  and the average fraction of  $\lambda = (69 \pm 5)$  % extracted with the Doppler asymmetry method was found to be in good agreement with the average fraction of  $\lambda = (65 \pm 5)$  % obtained using the spectroscopic method.

In order to estimate the counterpart to the semi-cold Dy transfer, namely the semi-cold Sn transfer, i.e. the fraction of transfer events, where the ground state of  $^{118}\text{Sn}$  was directly populated regardless of the excitation of  $^{160}\text{Dy}$ , we

could also use a more direct procedure: The probability for observing the  $2_1^+ \rightarrow 0^+$  transition in  $^{118}\text{Sn}$  in coincidence with the  $4_g^+ \rightarrow 2_g^+$  or  $6_g^+ \rightarrow 4_g^+$  decay in  $^{160}\text{Dy}$  is a direct measure of the probability that  $^{118}\text{Sn}$  was excited in the transfer process, as virtually all relevant excited states in  $^{118}\text{Sn}$  decay via the first excited  $2_1^+$  state and as the direct population of the  $2_g^+$  and  $0_g^+$  state in  $^{160}\text{Dy}$ , which are missed by our gating condition, is negligible small at reaction distances considered. The resulting efficiency corrected probability for the  $2_1^+ \rightarrow 0^+$  transition in  $^{118}\text{Sn}$  amount to  $(55 \pm 10)$  % of the total 2n pickup probability at these surface distances, which means that  $(45 \pm 10)$  % of the 2n transfer events lead to the  $0^+$  ground state of  $^{118}\text{Sn}$ . This surprisingly large number of semi-cold Sn transfer events as compared to semi-cold Dy transfer events of  $(7 \pm 3)$  % is corroborated by the result of the corresponding Doppler asymmetry analysis. This analysis results in a fraction of  $(43 \pm 10)$  % of the 2n pickup events which are not connected with a  $\gamma$ -ray of  $E_\gamma > 720$  keV from the decay of excited states in  $^{118}\text{Sn}$ , however, with the contribution of directly populated  $2_1^+$  states in  $^{118}\text{Sn}$  still included. Comparing this fraction with the fraction of directly populated  $0^+$  states in  $^{118}\text{Sn}$  determined above, the fraction of directly populated  $2_1^+$  states can be estimated to  $(-2 \pm 15)$  %, i.e. to  $\leq 15$  %, which is consistent within any reasonable transfer scenario. The semi-cold Dy and Sn transfer and their  $\Delta$ -dependence will be discussed in the next section.

### 3 Discussion of transfer probabilities

The population probability  $P_f$  for a specific final channel f in a quasi-elastic event q can be written within the semiclassical approximation as

$$P_f(\Delta) = \frac{d\sigma_f(\Delta(\theta_{cm}, E_0))}{d\Omega} / \frac{d\sigma_q(\Delta(\theta_{cm}, E_0))}{d\Omega} \quad (8)$$

where  $\frac{d\sigma_f(\Delta(\theta_{cm}, E_0))}{d\Omega}$  denotes the cross section for the final channel f and  $\frac{d\sigma_q(\Delta(\theta_{cm}, E_0))}{d\Omega}$  the quasi-elastic cross section, i.e. the fraction of the Rutherford cross section, which has escaped absorption into non quasi-elastic reaction channels.

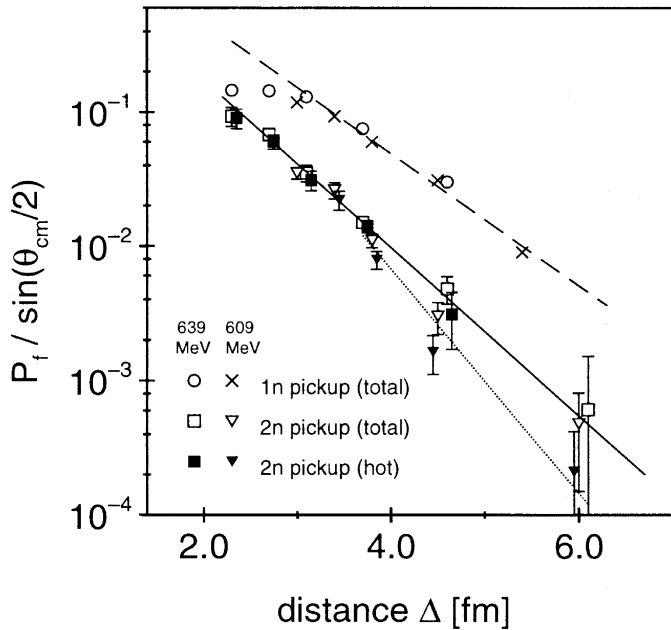


**Fig. 6.** Comparison of the total transfer probabilities for observing a 1n pickup event (circles and crosses) and a 2n pickup event (open squares and triangles). In addition to the hot 2n transfer probabilities, where at least one  $E_\gamma > 720$  keV  $\gamma$ -ray was detected (disregarding the  $2_1^+ \rightarrow 0^+$  transition in  $^{118}\text{Sn}$ ) are shown by filled squares and triangles. The circles and squares (crosses and triangles) are deduced from the measurement at a beam energy of 639 MeV (609 MeV)

The population probabilities for different transfer channels, corrected for the kinematic factor  $\sin(\theta_{\text{cm}}/2)$  (see below), are shown in Fig. 6 as a function of the surface distance  $\Delta$ . The open squares and the triangles represent the total 2n transfer probability  $P_{2n}(I \geq 4)$  deduced from the  $4_g^+ \rightarrow 2_g^+$  transition in  $^{160}\text{Dy}$  at two different beam energies of 639 MeV and 609 MeV, respectively. These 2n transfer probabilities are in good agreement with values extracted by Kernan et al. [4], who also investigated the system  $^{162}\text{Dy}(^{116}\text{Sn}, ^{118}\text{Sn})^{160}\text{Dy}$  at similar beam energies. For distances below  $\Delta \approx 5$  fm, where it is possible to generate  $\gamma$ -sum energy vs.  $\gamma$ -multiplicity planes for the 2n pickup channel, the probability  $P_{2n}(I \geq 4)$  is a good measure for the total 2n pickup probability  $P_{2n}$  since the population of low spin states feeding directly to the  $2_g^+$  or  $0_g^+$  state can be shown to be negligible small (compare Fig. 3). At larger distances, however, an increasing fraction of events feeding directly the  $2_g^+$  or  $0_g^+$  state cannot be ruled out. Note, moreover, that at surface distances larger than  $\Delta \approx 4$  fm the probability for Coulomb excitation of the  $^{160}\text{Dy}$  target impurity ( $\approx 1.5 \cdot 10^{-3}$ ) starts to compete with the 2n transfer probability to  $^{160}\text{Dy}$ . The contribution from the Coulomb excitation of the  $^{160}\text{Dy}$  target impurity has been subtracted from the data shown in Fig. 6 and 7. Also plotted in Fig. 6 are the experimental values of the 1n pickup probability  $P_{1n}(I \geq 3/2)$  (circles and crosses), which were deduced from the lowest transition  $3/2^+ \rightarrow 1/2^+$  in  $^{117}\text{Sn}$  (see Fig. 2), which is

expected to represent at least a lower limit of the total 1n pickup probability  $P_{1n}$ ; a low lying isomer in  $^{117}\text{Sn}$  and direct transitions of low spin states to the ground state may cause an underestimation of the 1n pickup probability.

As long as the transfer probabilities are well below  $P_{\text{tr}} \approx 10\%$ , i.e. at distances  $\Delta$ , where the nuclear overlap is sufficient small, the 1n and 2n transfer probabilities are exponentially decreasing functions, as expected in the framework of the semiclassical tunneling model [18]. In this model, the transfer probability for  $x$  neutrons can be written as

$$P_{xn}(\Delta) / \sin(\theta_{\text{cm}}(\Delta)/2) \propto \exp(-2\alpha_{xn}\Delta), \quad (9)$$

where the slope  $\alpha$  is related to the reduced mass  $\mu$  of the transferred particle(s) (1n or 2n) and to the binding energy  $E_B$  of the neutron(s) with  $\alpha_{\text{th}} = \sqrt{2\mu E_B}/\hbar$ . The factor  $\sin(\theta_{\text{cm}}/2)$  results from the fact, that the contact time and thereby the tunneling probability at the distance of closest approach is changing with kinematics. Since the mass transfer is small compared to the masses of the initial nuclei and also the structure of the initial and final nuclei are rather similar, the slope of the 2n transfer  $\alpha_{2n}$  should be approximately twice the slope of the 1n transfer  $\alpha_{1n}$ , no matter whether the transfer of two independent neutrons (uncorrelated pair transfer) or of a correlated neutron pair (correlated pair transfer) is considered. As known already from previous 2n transfer studies on deformed heavy nuclei, however, the slope of the 1n and 2n pickup behave quite differently: While the measured slope of the 1n pickup with  $\alpha_{1n} = (0.56 \pm 0.03) \text{ fm}^{-1}$  lies close to the expected value of  $\alpha_{\text{th}} = 0.53 \text{ fm}^{-1}$  (using a binding energy of  $E_B = 6$  MeV), the observed slope of the 2n pickup with  $\alpha_{2n} = (0.72 \pm 0.05) \text{ fm}^{-1}$  is too flat. This observation is usually referred to as slope anomaly [14, 16, 19]. Wu et al. [14] and more recently Develin et al. [5] suggested that this anomaly might be caused by the cold component of the 2n transfer. Indeed, when selecting hot transfer events by requiring at least one  $\gamma$ -ray with an energy of  $E_\gamma > 720$  keV (disregarding the  $2_1^+ \rightarrow 0^+$  transition in  $^{118}\text{Sn}$ ), the resulting efficiency corrected 2n pickup probabilities (shown in Fig. 6 by the filled symbols) exhibit a steeper slope for  $\Delta > 3.5$  fm. The resulting slope parameter of  $\alpha_{2n}^{\text{hot}} = (1.0 \pm 0.2) \text{ fm}^{-1}$  is close to the expected one of  $\alpha_{2n} \approx 2\alpha_{1n} = (1.12 \pm 0.06) \text{ fm}^{-1}$ . At distances of  $2.3 \text{ fm} \leq \Delta \leq 3.8 \text{ fm}$ , which were used in the previous sections to demonstrate our analysis methods, the hot transfer exhausts  $\geq 95\%$  of the total 2n transfer probability, that is the cold 2n pickup probability is less than 5%, in agreement with the result of section 2.2. At distances  $\Delta \gtrsim 3.5$  fm, however, the fraction of cold events seems to increase significantly.

Although the statistics of our present experiment does not allow to extract the  $\Delta$ -dependence of the true cold 2n pickup probabilities, it is sufficient to determine the surface distance dependence of the semi-cold events. Figure 7 shows in addition to the total 2n pickup probabilities (open symbols) the semi-cold Dy 2n pickup probabilities (filled symbols). Regarding both probabilities, it is obvious, that the fraction of 2n transfer events populating

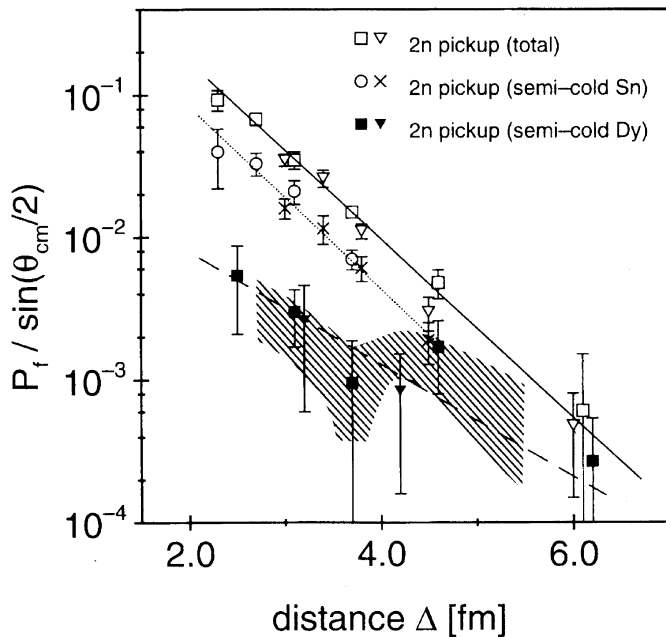


**Fig. 7.** Comparison of the total probabilities for observing a 2n pickup event and the semi-cold Sn and Dy 2n pickup probabilities determined at two different beam energies (see also Fig. 6). The hatched area shows the results obtained by the authors of [4] for the 'cold' 2n pickup probabilities using a different selection criterion

directly the yrast sequence in the deformed  $^{160}\text{Dy}$  transfer products shows a large  $\Delta$  dependence; from  $\Delta = 2.3$  fm up to  $\Delta = 6.3$  fm this fraction increases from  $\approx 7\%$  up to almost 50%, but at the same time the absolute semi-cold Dy pickup probability is reduced by a factor of about 50. This behaviour seems to be independent from the excitation of the  $^{118}\text{Sn}$  partner, as we found no evidence for a change when demanding explicitly the excitation of the  $2_1^+$  state in  $^{118}\text{Sn}$  or not. Our values for the magnitude and  $\Delta$  dependence of the semi-cold Dy 2n transfer probabilities are in agreement with the corresponding results of Kernan et al. [4] (hatched area in Fig. 7), although their selection criterion for cold events differs from ours. In particular, we explicitly retain also the cold high spin events which should get increasingly important at smaller surface distances. Remarkably enough, the two experiments seem to agree even at small surface distances which might be somewhat fortuitous. The present result, however, proves that the decrease of the fraction of semi-cold events at  $\Delta \leq 4$  fm, responsible for the considerable shallower  $\Delta$ -dependence of this class of events, is not due to the neglect of the high spin yrast states as suggested by Devlin et al. [5] in view of the data of [4], but must be caused by the 2n transfer mechanism itself.

Also shown in Fig. 7 are the probabilities for semi-cold Sn 2n pickup events. The semi-cold Sn and Dy 2n transfer probabilities obviously exhibit a completely different behaviour. While the fraction of semi-cold Dy transfer events of the 2n pickup events increase with increasing  $\Delta$ , the fraction of semi-cold Sn transfer events is almost indepen-

dent of the surface distance  $\Delta$ , keeping an average value of  $(45 \pm 10)\%$ .

It is remarkable, that the present semi-cold Sn pickup probabilities involving a deformed collision partner behave similarly in absolute and relative magnitude to the corresponding probabilities observed in collisions with spherical Sn-isotopes [4, 7] if compared at similar surface distances. It looks as if the semi-cold Sn events, where one sums over the cold and (dominating) hot final states in the remaining donor nuclei, are independent of where the two picked-up neutrons come from, i.e. that the probability of the Sn nucleus to end up in the ground state after a 2n pickup does not depend on the structure of the donor nuclei nor — as reflected in the constancy of the semi-cold fraction on  $\Delta$  — on the spin and excitation energy of the donor before the transfer. This observation underlines that one has to study (true) cold events in order to be able to extract in these investigations information about the pairing correlation in the ground states or ground state bands of the participating nuclei.

Considering now the semi-cold Dy events, their unexpected shallow slope as compared to the semi-cold Sn events seems to point at the deformation of the Dy nuclei as the possible origin of this behaviour. Indeed, when considering deformation effects in transfer calculations, namely the increased importance of higher transfer multipolarities as suggested by calculations of Landowne et al. [11], distinct modifications of the population pattern of the  $^{160}\text{Dy}$  transfer product are predicted, in particular a strong reduction of the cross section for populating the yrast sequence in  $^{160}\text{Dy}$  with decreasing surface distance  $\Delta$ . The predicted oscillations of the cold cross sections leading to low spin yrast states in  $^{160}\text{Dy}$ , however, should not be visible in our data, as we are summing over all populated yrast states. On the other hand, the result of Kernan et al. [4], which is restricted to final spin values  $\leq 10\hbar$ , seems to reflect a structure, which in fact has been interpreted by the authors of [4] as evidence for the oscillatory behaviour predicted by Landowne et al. Unfortunately, our present data is not yet accurately enough to make a sensible contribution to this issue; our data is not in contradiction with the result of [4] although we would have to assume in this case that the contribution from yrast states with  $I > 10^+$  to the semi-cold Dy transfer are considerably smaller than expected. A new experiment, where the Crystal Ball has been extended by 5 Ge EUROBALL CLUSTER detectors with a total photo peak efficiency of  $\varepsilon_{\text{Ph}}(E_\gamma = 1.3 \text{ MeV}) \approx 2\%$ , dedicated to investigate this effect in more detail is presently being analysed [20].

## 4 Conclusion

The present investigation performed with the  $^{162}\text{Dy}(^{116}\text{Sn}, ^{118}\text{Sn})^{160}\text{Dy}$  reaction has demonstrated the feasibility to study cold transfer events in collisions between spherical and deformed heavy nuclei using a highly  $\gamma$ -efficient  $4\pi$  scintillator array together with a heavy ion detector system to select binary events and high resolution Ge-detectors for final channel selection.

However, as the ratio of the cold to the total 2n transfer events turned out to be as small as 3 %, the overall Ge-efficiency of the present setup was not yet sufficient for a more detailed study of these cold transfer events, but allowed only to investigate semi-cold Sn and Dy 2n transfer probabilities, i.e. to select 2n transfer events where either the Sn or Dy nucleus stays in the ground state or yrast band, respectively, while the excitation of the transfer partner is disregarded. By increasing the Ge-efficiency by at least an order of magnitude it should be possible to study also the cold 2n transfer probabilities for individual final states as a function of the surface distance  $\Delta$ .

The semi-cold 2n transfer probabilities are obviously rather insensitive to the structure of the other transfer partner and do not seem to depend on the excitation energy or spin of the latter at the moment the transfer process takes place. On the other hand, the probabilities for semi-cold transfer events seem to depend strongly on the deformation of the considered isotopes: While the fraction of semi-cold Sn 2n pickups as compared to the total 2n pickup events is large ( $45 \pm 10$  %) and constant over the measured range of surface distances, the corresponding fraction of semi-cold Dy events decreases from approximately 50 % at  $\Delta \approx 6$  fm to about 7 % at  $\Delta \approx 2.8$  fm. The large number at large distances is similar to the Sn value and might indeed suggest pairing correlations also for the system  $^{162}\text{Dy}(^{116}\text{Sn}, ^{118}\text{Sn})^{160}\text{Dy}$  as proposed by the authors of [2–4]. We have shown that this decrease of the semi-cold Dy fraction is not due to a high spin cut off caused by our selection criteria for cold events but has to be traced back to the transfer mechanism itself. In fact, the shallow  $\Delta$ -dependence of the semi-cold Dy events is qualitatively explained by including also higher transfer multipolarities in the calculations [11] which gain their strong influence on the transfer probabilities from the large deformation of the Dy nuclei. It is obvious that these strong modifications of the transfer probabilities caused by the deformation have to be studied in detail experimentally as well as theoretically before one can start to investigate

further effects like the influence of the rotation on the transfer process.

We would like to thank the accelerator crew of the Max-Planck-Institut für Kernphysik for the excellent  $^{116}\text{Sn}$  beam, and Dr. F. Köck and Dr. Ch. Ender for their continuous help in keeping electronics and data acquisition of the Crystal Ball in good shape.

## References

1. W. v. Oertzen, Inst. Phys. Conf. Ser. No 110: Section 2, 133 (1990)
2. C. Y. Wu et al., Ann. Rev. Nucl. Part. Sci. **40**, 285 (1990)
3. D. Cline, Nucl. Phys. **A520**, 493c (1990)
4. W. J. Kernan et al., Nucl. Phys. **A524**, 344 (1991)
5. M. Devlin et al., Phys. Rev. **C53**, 2900 (1996)
6. K. Dietrich, Ann. Phys. **66**, 480 (1971)
7. W. v. Oertzen et al., Z. Phys. **A326**, 463 (1987)
8. H. Weiss, Phys. Rev. **C19**, 834 (1979)
9. M. W. Guidry et al., Nucl. Phys. **A361**, 275 (1981)
10. D. Schwalm: Coulomb excitation at safe and unsafe energies, in: Probing the Nuclear Paradigm with Heavy Ion Reactions, The Science and Culture Series Physics, Vol. 8, edited by R. A. Broglia, P. Kienle, R. F. Bortignon (World Scientific, Singapore) 1995, p. 1.
11. S. Landowne et al., Nucl. Phys. **A484**, 98 (1988)
12. K. A. Erb et al., Phys. Rev. Lett. **33**, 1102 (1974)
13. D. L. Hanson et al., Nucl. Phys. **A269**, 520 (1976)
14. C. Y. Wu et al., Phys. Rev. **C39**, 298 (1989)
15. V. Metag et al., Comm. Nucl. Part. Phys. **16**, 213 (1986)
16. F. W. N. de Boer et al., Z. Phys **A325**, 457 (1986)
17. T. Härtlein, Ph.D. thesis Universität Heidelberg (1994)
18. R. Bass, Nuclear Reactions with Heavy Ions (Springer Verlag, Berlin – Heidelberg – New York, 1980)
19. A. O. Macciavelli et al., Nucl. Phys. **A432**, 436 (1985)
20. H. Bauer et al., to be published